Biomaterials 31 (2010) 1655–1665

Contents lists available at ScienceDirect

Biomaterials

journal homepage: www.elsevier.com/locate/biomaterials

Cross-linked open-pore elastic hydrogels based on tropoelastin, elastin and high pressure CO_2

Nasim Annabi [a], Suzanne M. Mithieux [b], Anthony S. Weiss [b], Fariba Dehghani [a,*]

[a] School of Chemical and Biomolecular Engineering, The University of Sydney, Sydney, NSW 2006, Australia
[b] School of Molecular and Microbial Biosciences, The University of Sydney, Sydney, NSW 2006, Australia

ARTICLE INFO

Article history:
Received 16 October 2009
Accepted 17 November 2009
Available online 6 December 2009

Keywords:
Tropoelastin
α-Elastin
Hydrogel
Glutaraldehyde
High pressure CO_2
Fibroblast

ABSTRACT

In this study the effect of high pressure CO_2 on the synthesis and characteristics of elastin-based hybrid hydrogels was investigated. Tropoelastin/α-elastin hybrid hydrogels were fabricated by chemically cross-linking tropoelastin/α-elastin solutions with glutaraldehyde at high pressure CO_2. Dense gas CO_2 had a significant impact on the characteristics of the fabricated hydrogels including porosity, swelling ratio, compressive properties, and modulus of elasticity. Compared to fabrication at atmospheric pressure high pressure CO_2 based construction eliminated the skin-like formation on the top surfaces of hydrogels and generated larger pores with an average pore size of 78 ± 17 μm. The swelling ratios of composite hydrogels fabricated at high pressure CO_2 were lower than the gels produced at atmospheric pressure as a result of a higher degree of cross-linking. Dense gas CO_2 substantially increased the mechanical properties of fabricated hydrogels. The compressive and tensile modulus of 50/50 weight ratio tropoelastin/α-elastin composite hydrogels were enhanced 2 and 2.5 fold, respectively, when the pressure was increased from 1 to 60 bar. *In vitro* studies show that the presence of large pores throughout the hydrogel matrix fabricated at high pressure CO_2 enabled the migration of human skin fibroblast cells 300 μm into the construct.

1. Introduction

Tissue engineering offers the potential to create functional and viable tissue constructs for patients requiring organ replacement [1]. A three dimensional (3D) scaffold is necessary to serve as a template to guide cell growth and tissue development. The chemical composition, mechanical properties, porosity, pore interconnectivity, and 3D structures of the scaffold greatly influence the formation of the new tissue [2]. Hydrogels have emerged as leading candidates for engineered tissue scaffolds as much of the native extracellular matrix (ECM) in the body forms hydrated polymeric networks that closely resemble the mechanical, biological and physical properties of hydrogels [3]. Hydrogels composed of natural polymers, such as collagen, hyaluronan (HA), fibrin, alginate, agarose, dextran, chitosan, and elastin-like polypeptides (ELPs), are desirable for tissue engineering due to their similarities with the extracellular matrix, high chemical versatility, typically good biological performance and inherent cellular interaction [4].

Elastin is an insoluble, polymeric, ECM protein that provides various tissues in the body with the properties of extensibility and elastic recoil [5]. Elastin-based biomaterials are increasingly investigated due to their remarkable properties such as elasticity, self-assembly, long-term stability, and biological activity [6]. Elastin is highly insoluble as a consequence of extensive lysine mediated cross-linking and therefore difficult to process into new biomaterials. Consequently, soluble forms of elastin including α-elastin [7–9], recombinant tropoelastin (rTE) [10,11], and engineered recombinant elastin-like polypeptides (ELPs) [12] are frequently used to form cross-linked hydrogels. Tropoelastin is the soluble precursor of elastin, and α-elastin is an oxalic acid-solubilised derivation of elastin [13]. rTE has been chemically cross-linked to form synthetic elastin (SE) hydrogels [11]. The fabricated SE hydrogels had strength, elasticity, and biocompatibility properties similar to those of naturally occurring human elastic tissue. *In vitro* and *in vivo* experiments revealed that these SE hydrogels could support cellular growth; however, the non-homogenous and limited porosity of these constructs prohibited cellular migration deep into the hydrogels. Generally, this lack of cellular migration into the 3D structures due to the existence of a discrete discontinuous pore network is an issue associated with the current approaches used for SE hydrogel fabrication. Electrospinnig techniques [14] and dense gas carbon dioxide (CO_2) [7,9] have been used to facilitate greater cell penetration and infiltration into the 3D structure of elastin-based biomaterials.

* Corresponding author.
E-mail address: fdehghani@usyd.edu.au (F. Dehghani).

0142-9612/$ – see front matter © 2009 Elsevier Ltd. All rights reserved.
doi:10.1016/j.biomaterials.2009.11.051

Dense gas CO_2 has been used widely as an attractive means of producing porous biomaterials for tissue engineering applications [15,16]. It has been exploited as a foaming agent to induce porosity in the structure of several common hydrophobic polymers such as poly (lactic acid) (PLA), poly (lactic acid-co-glycolic acid) (PLGA), and polycaprolactone (PCL) [15–18]. However, dense gas CO_2 generally has low solubility in hydrophilic polymers. Various techniques such as CO_2-water emulsion templating [19–23] or the use of a co-solvent system have been developed to improve the ability of a dense gas to diffuse into a hydrophilic polymer and produce porosity [24,25]. Hydrogels fabricated using these techniques generally contain small pores with the average pore size less than 26 μm and display limited porosity [20,21].

The results of our previous studies demonstrate that highly interconnected pores with thin walled structures resembling natural elastin can be produced by cross-linking α-elastin using glutaraldehyde (GA) under high pressure CO_2 [9]. The cell infiltration throughout the hydrogels was considerably enhanced compared with the samples produced at atmospheric conditions. This improvement resulted from CO_2 induced channels within the structure of the α-elastin hydrogels [9]. However, the low number of lysine residues (less than 1%) in α-elastin resulted in limited cross-linking with GA and consequently poor mechanical integrity [26]. The use of a cross-linking agent such as hexamethylene diisocyanate (HMDI) that can react with other amino acids available in the α-elastin structure increased the cross-linking density and mechanical properties of fabricated hydrogels [7]. The reaction was undertaken in a CO_2 expanded dimethyl sulfoxide (DMSO) solution and required solvent residue removal after the process. *In vitro* studies demonstrated that the fabricated constructs promoted cellular migration and growth throughout the 3D matrix [7].

The objective of this study was to fabricate a composite recombinant rTE/α-elastin hydrogel in an aqueous based system with desirable properties for tissue engineering applications. The addition of rTE containing 35 lysine residues per molecule to the protein solution was expected to increase the cross-linking density and promote the mechanical properties of elastin-based hydrogels. The effect of pressure, rTE and GA concentrations on the characteristics of hybrid hydrogels were investigated. *In vitro* studies were conducted to assess the cellular growth and proliferation in the 3D structures of fabricated hydrogels.

2. Materials and methods

2.1. Materials

rTE isoform SHELΔ26A (Synthetic Human Elastin without domain 26A) corresponding to amino acid residues 27–724 of GenBank entry AAC98394 (gi 182020) was purified from bacteria on a multi-gram scale as previously described [27]. α-elastin extracted from bovine ligament was obtained from Elastin Products Co. (Missouri USA). GA was purchased from Sigma. Food grade carbon dioxide (99.99% purity) was supplied by BOC. GM3348 fibroblast cell line was obtained from the Coriell Cell Repository. Cells were maintained in Dulbecco's Modified Eagle's Medium (DMEM) supplemented with 10% v/v fetal bovine serum (FBS), penicillin and streptomycin. All tissue culture reagents were obtained from Sigma.

2.2. Hydrogel formation

2.2.1. Hydrogel fabrication at atmospheric pressure

In each experiment a 100 mg/ml of rTE/α-elastin in PBS (150 mM NaCl) was mixed with GA at 4 °C and the solution was immediately pipetted into a Lab-Tek chamber slide. The slide was then placed at 37 °C for 24 h to fabricate a hydrogel. The cross-linked hydrogel was removed from the slide, washed repeatedly with PBS, and stored in PBS for characterisation.

A preliminary set of experiments were conducted to determine the required ratio of GA and rTE/α-elastin solution for the hydrogel fabrication. A 50/50 weight ratio rTE/α-elastin was used to optimise the concentration of GA and protein solution. The concentration of rTE/α-elastin (50/50) solution was varied between 5 mg/ml and 100 mg/ml, and GA between 0.05 and 0.5% (v/v). The solutions were pipetted into a Lab-Tek chamber slide and then placed at 37 °C for 24 h. The cross-linked hydrogels were washed in PBS, then placed in 100 mM Tris ($(HOCH_2)_3CNH_2$) in PBS for 1 h to inhibit further cross-linking and stored in PBS for characterisation.

2.2.2. Dense gas in hydrogel formation

The experimental procedure used to fabricate rTE/α-elastin hydrogels was similar to our previous study for the fabrication of cross-linked α-elastin hydrogel by the dense gas CO_2 [9]. Briefly, rTE/α-elastin solution containing GA was injected into a custom-made Teflon mould placed inside the high pressure vessel. After the vessel was sealed and approached thermal equilibrium at 37 °C, the system was pressurised with CO_2 to 60 bar, isolated and maintained at these conditions for a set period of time. The system was then depressurised and the sample was collected. Cross-linked structures were immediately washed repeatedly in PBS, and then placed in 100 mM Tris in PBS for 1 h. After Tris treatment, the hydrogels were washed twice and stored in PBS for further analysis.

The effects of reaction time, cross-linker concentration, depressurisation rate, and rTE concentration on the characteristics of hydrogels were assessed. Different concentrations of GA (i.e. 0.25 and 0.5%(v/v)) were mixed with 100 mg/ml of rTE/α-elastin (50/50) and the solutions were pipetted into the mould, containing two individual wells and placed inside the high pressure vessel. The system was then pressurised to 60 bar for a certain period of time. Different rates of depressurisation were used in order to investigate the effect of depressurisation rate on the properties of fabricated hydrogels. The effect of addition of rTE on the characteristics of the hydrogels was investigated by using weight ratios of 25/75, 50/50, 75/25, and 100/0 rTE/α-elastin. All samples were prepared over a 1 h reaction time as our preliminary results demonstrated that the rigidity of fabricated hydrogels at high pressure was not significantly improved by keep increasing the reaction time.

2.3. Swelling properties

The swelling behaviour of the GA cross-linked rTE/α-elastin hydrogels produced at high pressure and atmospheric conditions was evaluated at two different temperatures (37 °C and 4 °C) in PBS. The hydrogels were lyophilised prior to use and were weighed dry. The samples were then swelled in 10 ml PBS for 24 h. For each temperature, at least three samples were tested. The excess liquid was removed from the swelled samples and the swelling ratio was calculated based on a ratio of the increase in mass to that of the dry sample.

2.4. Scanning electron microscopy (SEM)

The SEM images of samples were obtained using a Philips XL30 scanning electron microscope (15 KV) to determine the pore characteristics of the fabricated hydrogels and to examine cellular infiltration and adhesion. Lyophilised α-elastin hydrogels were mounted on aluminium stubs using conductive carbon paint, then gold coated prior to SEM analysis.

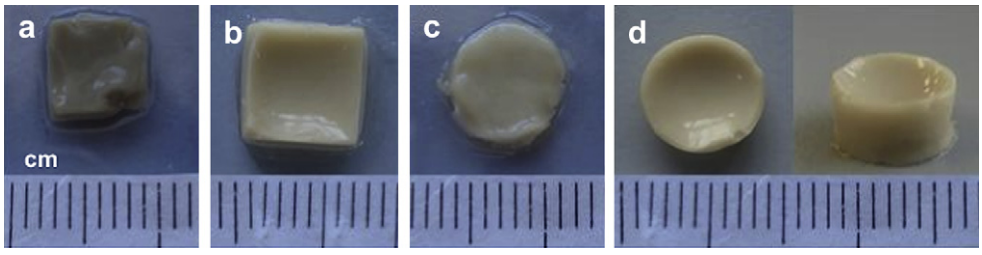

Fig. 1. GA cross-linked rTE/α-elastin hydrogels produced at (a, b) atmospheric condition, and (c, d) high pressure CO_2 (0.25% (v/v) GA was used in a, c and 0.5% (v/v) GA in b and d).

Cell-seeded hydrogels were fixed with 2% (v/v) GA in 0.1 M Na-cacodylate buffer with 0.1 M sucrose for 1 h at 37 °C. Samples underwent post-fixation with 1% osmium in 0.1 M Na-cacodylate for 1 h and were then dehydrated in ethanol solutions at 70%, 80%, 90% and 3 times 100% for 10 min each. For drying, the samples were immersed for 3 min in 100% hexamethyldisilazane (HMDS) then transferred to a desiccator for 25 min to avoid water contamination. Finally they were mounted on stubs and sputter coated with 10 nm gold.

2.5. Mechanical characterisation

2.5.1. Compressive properties

Uniaxial compression tests were performed in an unconfined state using a Bose ELF3400 mechanical tester with a 50 N load cell. The testing procedure as described previously [28–30]. Prior to mechanical testing, the hydrogels produced at high pressure CO_2 and atmospheric conditions were swelled for 2 h in PBS. The thickness

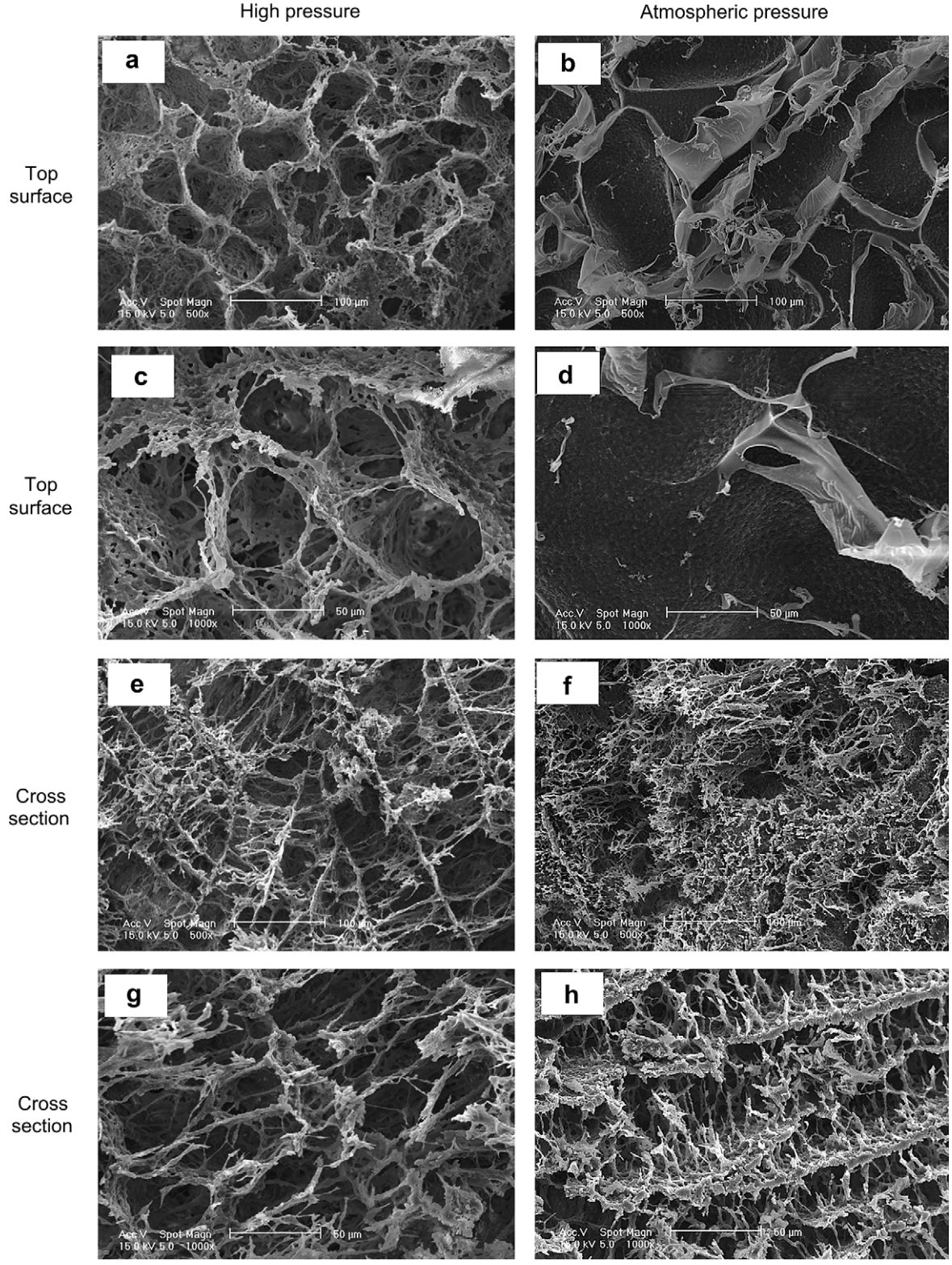

Fig. 2. SEM images of rTE/α-elastin hydrogels fabricated at (a, c, e, and g) 60 bar CO_2 pressure, and (b, d, f, and h) atmospheric pressure. Top surface of the samples are shown in images a–d and cross-sections in images e–h.

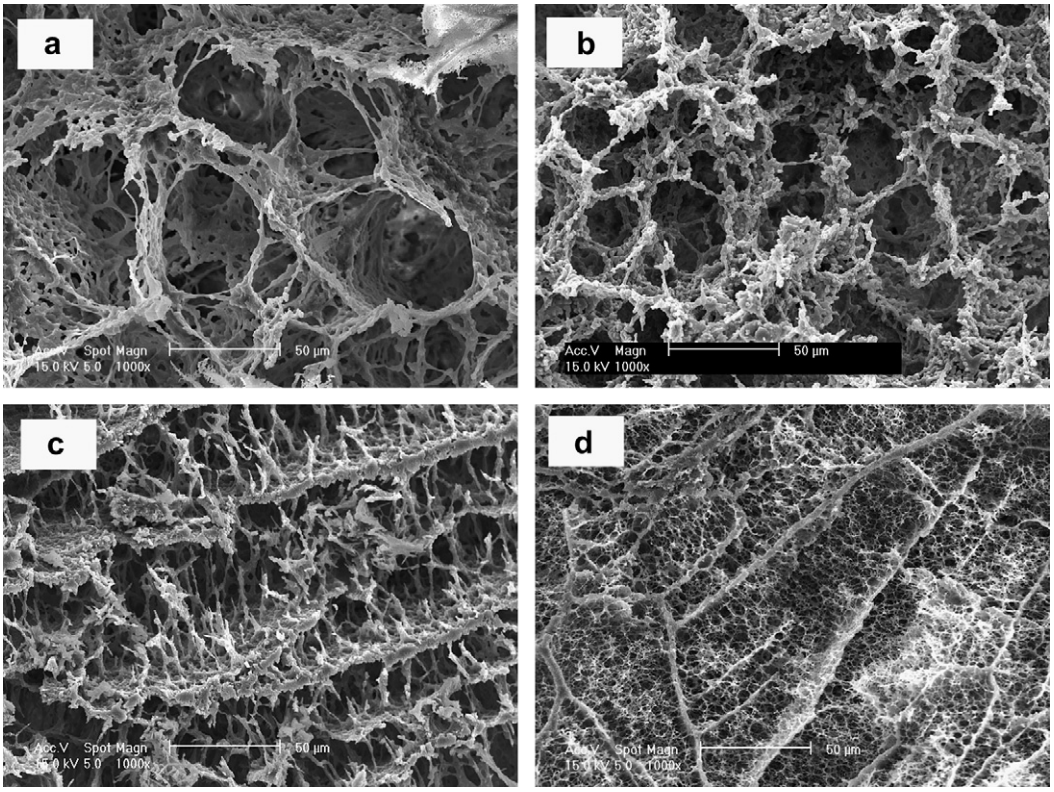

Fig. 3. SEM images of rTE/α-elastin hydrogels generated at (a,b) 60 bar pressure (60 bar/min depressurisation rate was used) and (c,d) atmospheric pressure. (0.25% (v/v) GA was used in a, c and 0.5% (v/v) in b and d).

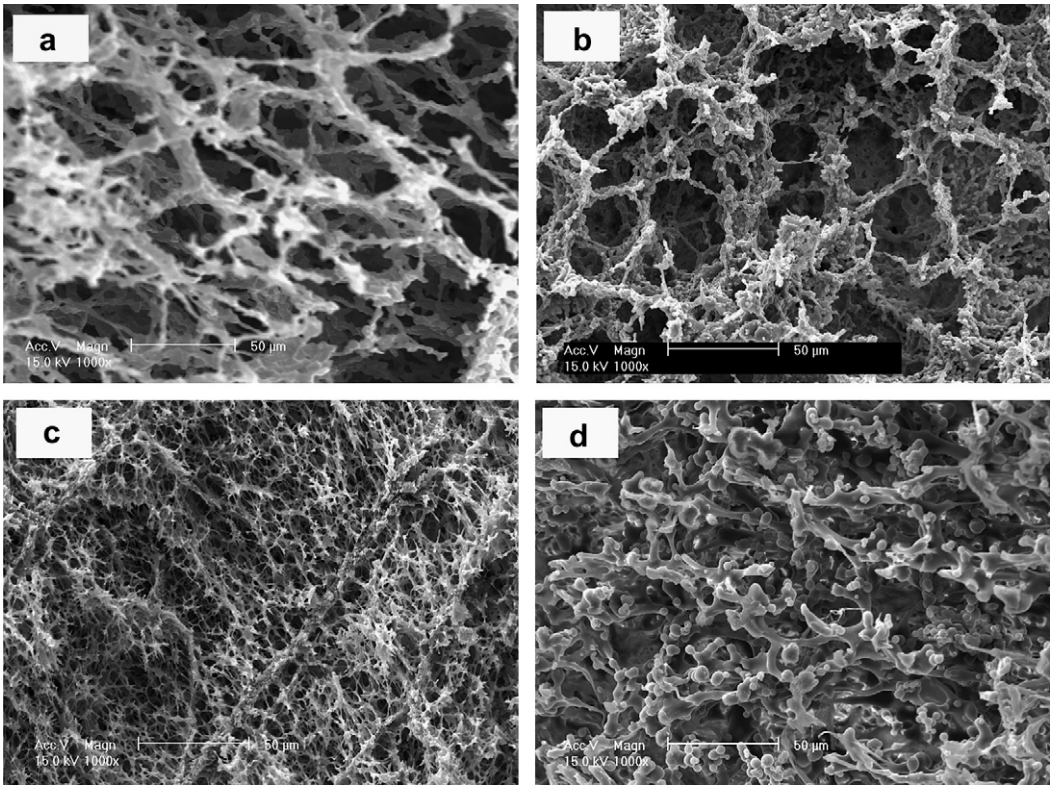

Fig. 4. SEM images of rTE/α-elastin composite hydrogels produced at 60 bar using (a) 25/75, (b) 50/50, (c) 75/25, and (d) 100/0 weight ratios of rTE/α-elastin (60 bar/min depressurisation rate was used).

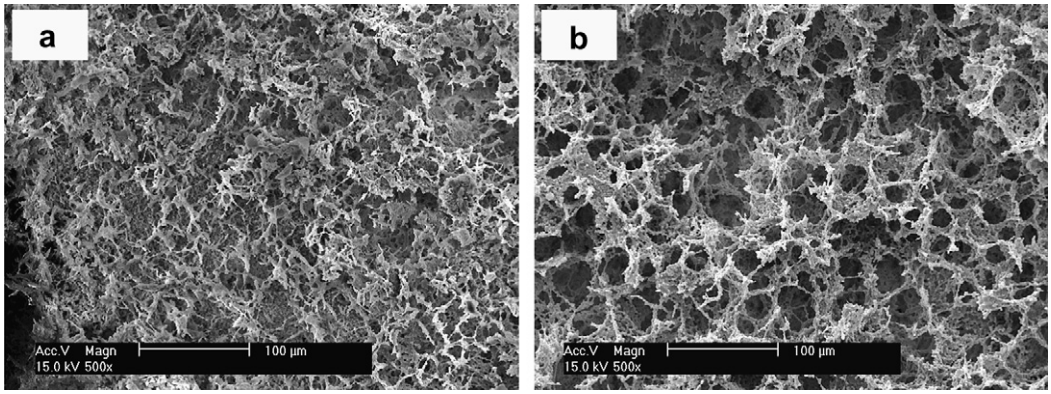

Fig. 5. SEM images of 0.5% GA cross-linked rTE/α-elastin (50/50) hydrogels produced at high pressure CO_2 using (a) slow depressurisation (1 bar/min), (b) fast depressurisation (60 bar/min).

(3 ± 0.1 mm) and diameter (12.5 ± 0.7 mm) of each sample was then measured using digital callipers. The compressive properties of the samples were tested in the hydrated state, in PBS, at room temperature. Compression (mm) and load (N) were recorded using Wintest software at a cross speed of 30 µm/s and 60% strain level. The samples were cyclically preconditioned for 7 cycles. The hydrogels were subsequently subjected to another loading and unloading cycle (8th cycle) where compression (mm) and load (N) were collected. The compressive modulus for the 8th cycle was obtained as the tangent slope of the stress-strain curve. In addition, the energy loss based on the 8th compression cycle was computed. Three specimens were tested for each sample type (sample produced at high pressure CO_2 or atmospheric pressure). The effect of rTE concentration on compressive modulus of the composite hydrogels was also investigated by using weight ratios of 25/75, 50/50, and 100/0 rTE/α-elastin.

2.5.2. Tensile properties

Tensile properties of GA cross-linked composite hydrogels were assessed in PBS at 37 °C using an Instron (Model 5543) tensile testing machine with a 50 N load cell. The samples were 30 ± 0.6 mm in length, 4 ± 0.1 mm in width, and 2 ± 0.05 mm in thickness. At each condition at least 3 samples were prepared for mechanical testing. The hydrogels were mounted onto the mechanical tester, with fine sand paper covering the grips to reduce slippage. Tensile tests were performed at a 3 mm/min strain rate until failure. The elasticity modulus was calculated as the tangent slope of the stress-strain curve. Maximum stress and strain were taken as the stress at failure and the corresponding strain level. The effect of rTE concentration on tensile properties of fabricated hydrogels was assessed.

2.6. In vitro cell culture

The ability of human skin fibroblast cells (GM3348) to grow into the hydrogels 3D structure was assessed. Following cross-linking, hydrogels were transferred into a 48-well plate and washed twice with ethanol to sterilise the materials. The hydrogels were then washed at least twice with culture media to remove any residual ethanol and equilibrated in culture media (DMEM, 10% FBS, pen-strep) at 37 °C overnight. The cells were then seeded onto the hydrogels at 1.6×10^5 cells/well and compared with an unseeded hydrogel in an adjacent well. Cells were cultured in a CO_2 incubator for 3 days at 37 °C, after which the hydrogels were fixed to assess cell proliferation and infiltration using light microscopy and SEM analysis.

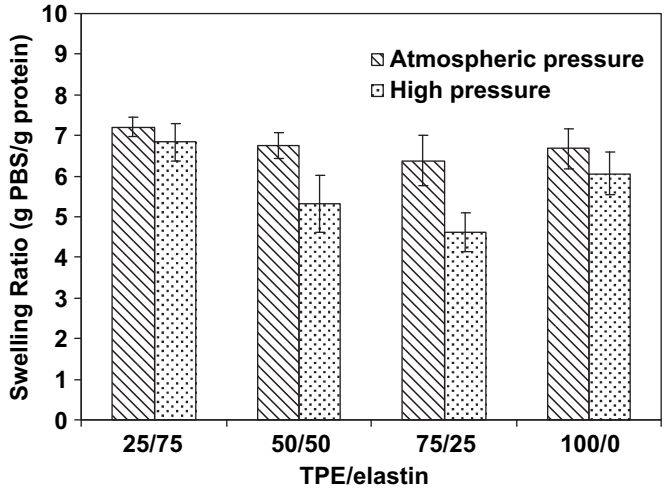

Fig. 6. Swelling behaviour of rTE/α-elastin hydrogels, produced at high pressure CO_2 and atmospheric condition, in PBS at 37 °C.

2.7. Light microscopy analysis on histological samples

The growth of the cells in fabricated hydrogels was confirmed using light microscopy analysis after fixing, sectioning, and staining cross-sections of cell-seeded scaffolds. The hydrogels containing cells were fixed by soaking in 10% formalin overnight. The scaffolds were then immersed in 70% ethanol. The samples were processed on an automated tissue processor on a 6 h cycle to paraffin through a graded series of ethanol, and xylene. They were embedded in paraffin wax and 5 µm sections were taken and collected onto glass slides and dried. The slides were then deparaffinised, rehydrated, stained using a standard haematoxylin and eosin staining procedure, dehydrated, cleared in xylene, and mounted in DPX. The cross-sections were examined using a light microscope (Olympus BX61) connected to a camera.

3. Results and discussions

3.1. Optimisation of protein and GA concentrations for hydrogel fabrication

Hydrogels were formed at atmospheric pressure when the GA and combined 50/50 rTE/α-elastin protein concentrations were above 0.1% (v/v) and 50 mg/ml, respectively. At low concentrations of GA and protein, soft films of cross-linked rTE/α-elastin formed at the bottom of the Lab-Tek chamber slides. Consequently, in this study 100 mg/ml of protein solution and two different cross-linker concentrations, 0.5 and 0.25% (v/v) GA, were used to produce hydrogels.

3.2. Visual observations of fabricated hybrid hydrogels

The addition of rTE to the protein solution had a substantial impact on the integrity of the fabricated hydrogels. All hybrid

Table 1
Swelling properties of hydrogels fabricated using high pressure CO_2.

rTE/α-elastin weight ratio	Swelling ratio (g PBS/g protein)	
	37 °C	4 °C
0/100	7 ± 3.2[a]	18.3 ± 4.6[a]
25/75	6.8 ± 0. 2	7.3 ± 0.4
50/50	5.3 ± 0.3	6.6 ± 1.9
75/25	4.6 ± 0.6	5.7 ± 0.3
100/0	6.1 ± 0.5	7.5 ± 0.6

[a] Data from Ref. [9].

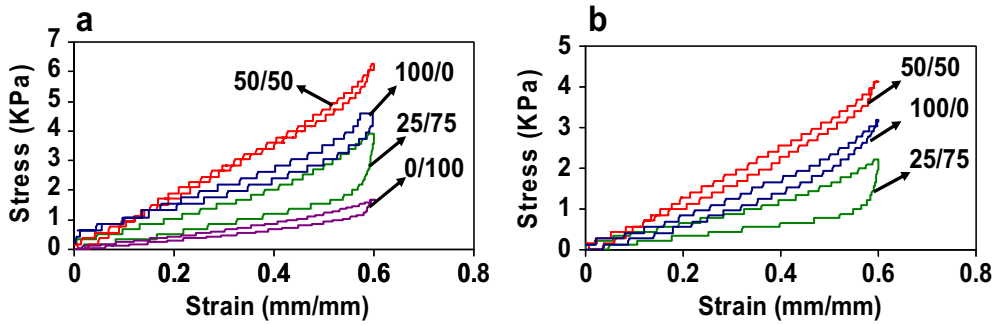

Fig. 7. Unconfined compressive behaviour of cross-linked composite hydrogels using deferent rTE/α-elastin hydrogels. Cyclic stress-strain data for the sample produced at (a) high pressure CO_2, and (b) atmospheric condition.

hydrogels produced by using rTE/α-elastin weight ratios greater than 50/50 were easily handled and kept their structure after swelling in PBS. However, 25/75 weight ratio rTE/α-elastin hydrogels were mechanically weak.

The visual observations of rTE/α-elastin hydrogels indicate that the mechanical integrity of fabricated hydrogels was improved by increasing both cross-linker concentrations and pressure. As indicated in Fig. 1, increasing the cross-linker concentrations from 0.25% (v/v) to 0.5% (v/v) and pressure from 1 bar to 60 bar resulted in the formation of more rigid hydrogels from 50/50 rTE/α-elastin solutions.

3.3. The pore structure of rTE/α-elastin hydrogels

The porosity and pore interconnectivity of the hydrogels play a critical role in tissue regeneration. The porosity allows for homogeneous cell distribution and growth within the 3D structures. Comparison of SEM images of GA cross-linked rTE/α-elastin (50/50) hydrogels in Fig. 2 indicates that the pore size of fabricated hydrogels increased when using high pressure CO_2. The presence of large pores in both the top surface (Fig. 2a and c) and cross section (Fig. 2e and g) of the sample fabricated at high pressure CO_2 using 0.25% (v/v) GA could facilitate cellular penetration and growth into the 3D structures. Equivalent circle diameters (ECD) of the pores were calculated using Image J software. The average pore size in the cross-sections of rTE/α-elastin hydrogels was enhanced as the pressure was increased from 1 bar to 60 bar. In hydrogels fabricated using dense gas CO_2 the pore sizes in the cross-sections were in the range of 22–55 μm with an average pore size of 35 ± 9 μm; however, the pore sizes in the cross-sections of the samples fabricated at atmospheric pressure were between 12 μm and 31 μm with an average pore size of 20 ± 5 μm. In addition, a skin layer was formed on the top surface of hybrid hydrogels produced at atmospheric conditions; however pores with average size of 78 ± 17 μm were formed on the top surface of hydrogels fabricated at high pressure CO_2. These pores were expected to allow for cell migration into the hydrogel matrices. This migration is prevented by the skin-like barrier on hydrogels produced at atmospheric conditions [9].

3.3.1. The effect of process parameters

Increasing the concentration of GA at both atmospheric and high pressures decreased the pore sizes of rTE/α-elastin hydrogels; this effect was more noticeable in the CO_2 system. As shown in Fig. 3, by increasing GA concentration from 0.25% (v/v) to 0.5% (v/v) the pore sizes for hydrogels produced at high pressure was decreased from 35 ± 9 μm (Fig. 3a) to 20 ± 5 μm (Fig. 3b), and for samples fabricated at atmospheric pressure pore size was decreased from 20 ± 5 μm (Fig. 3c) to 11 ± 2 μm (Fig. 3d).

The effect of rTE concentrations on pore morphology of hybrid hydrogels fabricated at high pressure CO_2 is shown in Fig. 4. The pores in pure rTE hydrogel (Fig. 4d) were much smaller and more densely packed compared to rTE/α-elastin hybrid hydrogels (Fig. 4a and b), demonstrating the substantial influence of rTE concentration on hydrogels microstructures.

Porosity is created in hydrogels fabricated with dense gas technology as a result of the release of CO_2 from the aqueous solution during depressurisation. The depressurisation rate had an impact on pore configuration. As shown in Fig. 5, larger pores were generated in the cross section of 50/50 rTE/α-elastin hydrogels cross-linked with 0.5% (v/v) GA at a depressurisation rate of 60 bar/min compared to 1 bar/min. At fast depressurisation rates large numbers of nuclei (bubbles) formed in the hydrogel matrix, increasing the chance of pore integration allowing for the subsequent formation of larger pores. Depressurisation rates greater than 60 bar/min were not practical as an overly rapid release of CO_2 from the matrix can cause high shear forces that rupture hydrogel integrity.

3.4. Swelling properties

The swelling properties of rTE/α-elastin hydrogels were measured in PBS at 37 °C and 4 °C. The swelling ratio of samples exposed to high pressure CO_2 was slightly lower than the hydrogels

Table 2
Mechanical characterisations of composite hydrogels produced at high pressure CO_2 and atmospheric conditions.

Sample	rTE/α-elastin weight ratio	Compressive modulus (KPa)	Energy loss (%)	Elastic modulus (KPa)	Stress at break (KPa)	Strain at break (%)
High pressure	**0/100**	1.9 ± 0.1[a]	–[b]	11.2 ± 2.3	4.3 ± 1.4	27.5 ± 0.7
	25/75	4.9 ± 0.7	47 ± 2.3	13.9 ± 3.6	5.6 ± 1.8	24 ± 2.7
	50/50	11.8 ± 1.7	2.5 ± 1.2	28.7 ± 2.1	8.4 ± 2.6	26.3 ± 6.7
	100/0	5.8 ± 0.3	23.1 ± 6.3	46.7 ± 2.6	39.3 ± 14.9	81.9 ± 32.9
Atmospheric pressure	**0/100**	–[b]	–[b]	–[b]	–[b]	–[b]
	25/75	2.3 ± 0.1	49.7 ± 10.2	8.2 ± 0.3	3.36 ± 0.2	40.9 ± 1.6
	50/50	6.1 ± 0.6	7.9 ± 3.1	11.5 ± 1.8	7.9 ± 0.7	64 ± 5.6
	100/0	4 ± 1.2	26.6 ± 4.6	32.7 ± 4.5	37.8 ± 20.9	92.5 ± 31.4

[a] Data from Ref. [26].
[b] Not determined.

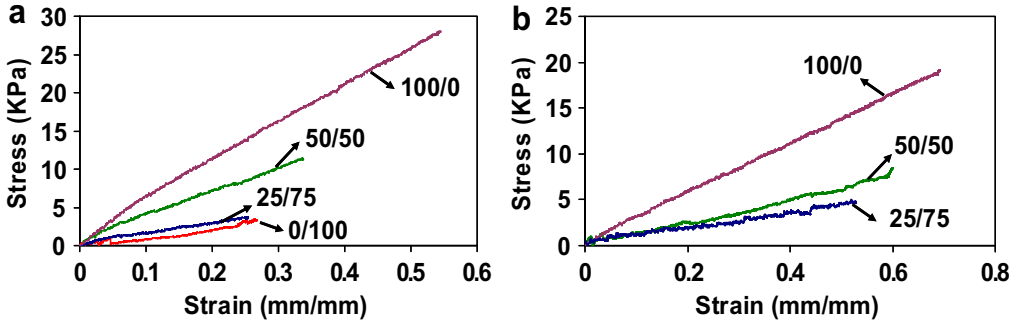

Fig. 8. Tensile properties of composite hydrogels produced at (a) high pressure CO_2, and (b) atmospheric condition.

fabricated at atmospheric conditions (Fig. 6). As indicated in Fig. 6 and Table 1, rTE concentrations had no significant effect on the swelling ratio of hydrogels. The hybrid hydrogels produced at high pressure CO_2 and atmospheric conditions exhibited swelling ratios in the range of 4.6–6.8 and 6.3–7.2 g PBS/g protein at 37 °C, respectively, when rTE/α-elastin ratios were changed from 25/75 to 100/0 weight ratio.

rTE/α-elastin hydrogels displayed stimuli-responsive characteristics toward temperature. Elevated temperature resulted in a contraction of the material due to water expulsion; therefore, the hydrogels swelled more at 4 °C compared with 37 °C as indicated in Table 1. The liquid uptake for all hybrid hydrogels produced at high pressure CO_2 increased on average 20 ± 8% when the temperature was lowered from 37 °C to 4 °C. For example, the PBS uptake of 50/50 rTE/α-elastin hydrogels cross-linked at high pressure CO_2 increased from 5.3 ± 0.3 to 7.3 ± 0.4 g PBS/g protein, when the temperature was decreased from 37 °C to 4 °C.

The swelling ratios of all the fabricated rTE/α-elastin hydrogels using high pressure CO_2 were lower than the swelling ratio of pure α-elastin hydrogels reported to be 19 ± 5 and 7 ± 3 g PBS/g protein at 4 °C and 37 °C, respectively [9].

3.5. Mechanical characterisation

3.5.1. Compressive properties

The compressive stress-strain curves of GA cross-linked rTE/α-elastin hydrogels produced at high pressure CO_2 and atmospheric condition are shown in Fig. 7. The stress-strain curves for all samples fabricated at high pressure CO_2 (Fig. 7a) and atmospheric pressure (Fig. 7b) were linear at 60% strain level, demonstrating the elasticity of fabricated hydrogels.

The compression modulus of the hydrogels produced at high pressure CO_2 was higher than those fabricated at atmospheric conditions, as indicated in Table 2. The compression modulus of 50/50 weight ratio rTE/α-elastin hydrogels was increased approximately 2-fold from 6.1 ± 0.6 kPa to 11.8 ± 1.7 kPa when the fabrication pressure was raised from 1 bar to 60 bar. This means that the samples produced at high pressure were stiffer than those produced at atmospheric conditions. As shown in our previous study, high pressure CO_2 facilitates coacervation [31]. This further increases the rate and degree of cross-linking in the polymer rich phase of the rTE/α-elastin/CO_2 solutions. Porosity is subsequently created by the release of the polymer lean CO_2 phase. Enhanced cross-linking in the polymer rich phase reduces the swelling ratio and increases the mechanical properties of hybrid hydrogels fabricated by dense gas CO_2.

The compressive properties of both hydrogels produced at high pressure CO_2 and atmospheric pressure were enhanced by increasing the rTE/α-elastin weight ratios. As shown in Table 2, the compression modulus of the GA cross-linked rTE/α-elastin hydrogels produced by high pressure CO_2 increased from 1.9 ± 0.1 to 4.9 ± 0.7 kPa and 11.8 ± 1.7 kPa when rTE/α-elastin weight ratios were increased from 0/100 to 25/75 and 50/50, respectively. The compressive modulus of hydrogels produced at atmospheric conditions increased from 2.4 ± 0.1 kPa to 6.1 ± 0.6 kPa when the rTE/α-elastin ratios was modified from 25/75 to 50/50, respectively. Pure α-elastin hydrogels (0/100), produced at atmospheric conditions, were fragile and had very weak mechanical strength; so it was not possible to measure their compressive properties. Pure cross-linked rTE hydrogels had lower compressive properties than hybrid hydrogels. The cross-links in elastin fragments are a hybrid, whereas rTE chemical cross-links are quite homogeneous. As a result, strength has been introduced to the α-elastin component in this process.

The compression properties of rTE/α-elastin hydrogels produced at high pressure CO_2 were higher than the compression modulus of α-elastin cross-linked with hexamethylene diisocyanate (HMDI) in our previous study (7 ± 1 kPa at 60% strain level) [9] demonstrating that rTE/α-elastin hydrogels were stiffer than HMDI cross-linked hydrogels.

The resilience of natural elastin allows for reversible deformation without loss of energy [32]. Energy loss is proportional to hysteresis. Generally, the energy loss for the composite hydrogels fabricated at high pressure CO_2 was slightly lower than the hydrogels produced at atmospheric conditions, demonstrating a small increase in hysteresis for the samples produced at atmospheric pressure. As indicated in Table 2, the 50/50 rTE/α-elastin hydrogels exhibited lowest energy loss at only 2.5 ± 1.2% and 7.9 ± 3.1% for the hydrogel produced at high pressure CO_2 and atmospheric pressure,

Table 3
Mechanical properties of elastin-based hydrogels and natural tissues.

Polymer networks	Cross-linking agent	E (kPa)	Ref[b]
rTE/α-elastin (using high pressure CO_2)	GA	11–47	Present study
rTE/α-elastin (using atmospheric pressure)	GA	3–33	Present study
Engineered ELP	GA	99–320	[43]
	HMDI	~50–1100	[44]
Engineered ELP	PQQ	250	[33]
Engineered ELP	BS3	80–700	[45]
α-elastin	EGDE	4–120	[8]
Engineered ELP	TSAT	1.6–15[a]	[46]
Engineered ELP	THPP	5.8–45.8[a]	[47]
Engineered ELP	tTG	0.28–1.7[a]	[38]
Recombinant human tropoelastin	BS3	220–280	[11]
Nucleus pulpous	–	11[a]	[48]
Natural aorta elastin	–	100–300	[49]

Abbreviations: E: Tensile modulus, ELP: elastin-like polypeptide, EGDE: ethylene glycol diglycidyl ether, PQQ: pyrroloquinoline quinine, TSAT: tris-succinimidyl aminotriacetate, THPP: β [tris(hydroxymethyl)phosphino]propionic acid, Ttg: tissue transglutaminase.

[a] Complex modulus.

[b] Some data estimated from graphical plots.

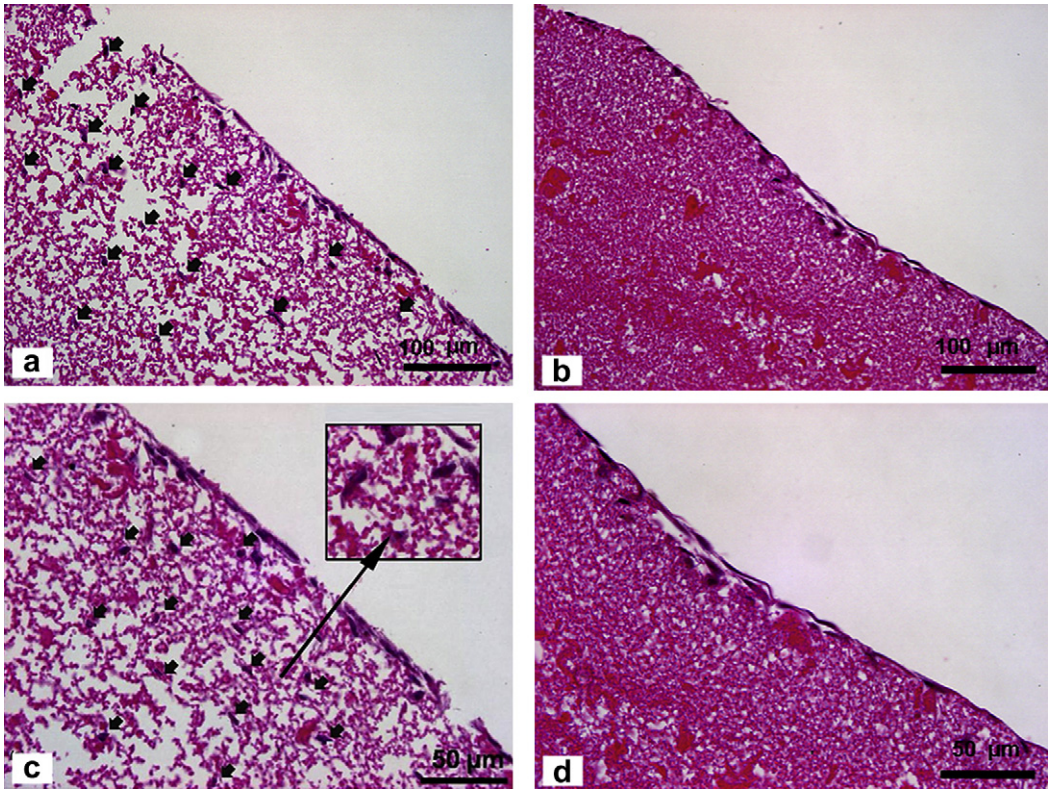

Fig. 9. Images of fibroblast cells cultured on a 50/50 rTE/α-elastin hydrogel produced at (a,c,) high pressure CO_2, and (b, d) atmospheric pressure. Arrowheads in the images show representative fibroblast cells.

respectively. The highest energy loss of 47 ± 2.3% and 49.7 ± 10.2% was observed for the 25/75 rTE/α-elastin hydrogels produced at high pressure CO_2 and atmospheric pressure, respectively. Pure rTE hydrogels (100/0) produced at both high pressure CO_2 and atmospheric pressure displayed comparable energy loss to purified native elastin reported to be 23 ± 10% [33].

The compressive modulus of the GA cross-linked rTE/α-elastin hydrogels was correlated with the swelling ratio. In general, samples with greater swelling have lower compressive moduli. This phenomenon has also been reported for a lysine diisocyanate (LDI) cross-linked ELP [28], a genipin cross-linked ELP [34], and a HMDI cross-linked α-elastin hydrogel [7].

3.5.2. Tensile properties

The tensile stress-strain curves of rTE/α-elastin hydrogels are shown in Fig. 8. As indicated in Table 2, the elastic modulus of hydrogels produced at high pressure CO_2 was increased 3.4-fold from 14 ± 4 kPa to 47 ± 3 kPa, when the rTE/α-elastin weight ratios was changed from 25/75 to 100/0, respectively. Hydrogels produced at high pressure CO_2 exhibited at least 1.5 times higher modulus of elasticity than those produced under atmospheric conditions. The elasticity modulus of hybrid hydrogels formed at atmospheric pressure was enhanced from 8.2 ± 0.3 kPa to 33 ± 5 kPa by increasing the weight ratios of rTE/α-elastin from 25/75 to 100/0, respectively. The pure α-elastin hydrogels (0/100) fabricated at atmospheric conditions were fragile and physically unstable, so that tensile testing was not possible.

In this study, an increase in the concentration of cross-linker and rTE resulted in an increase in the degree of cross-linking. While this led to a pore size reduction, the increased cross-linking density resulted in enhanced mechanical properties of fabricated hybrid hydrogels including compression and tensile modulus. The use of rTE provides a potential means for tailoring pore size and mechanical strength to those required for a specific tissue replacement application.

Tensile modulus of cross-linked biopolymers has also been correlated to the swelling ratio. Nickerson et al. found that a high level of swelling ratio in a cross-linked gelatin–maltodextrin hydrogel corresponded to a decrease in the tensile modulus of the hydrogel [35]. The tensile properties of hydrogels fabricated by dense gas CO_2 was consistent with the swelling properties, which showed a lower swelling ratio compared to hydrogels formed at atmospheric pressure.

The mechanical properties of hybrid hydrogels produced at high pressure CO_2 were compared with other elastin-based hydrogels fabricated using various cross-linkers (Table 3). As shown in Table 3, the tensile modulus of cross-linked rTE/α-elastin hydrogels produced at high pressure CO_2 is comparable to those reported in the literature for a number of elastin-based biomaterials and natural tissues. The tensile modulus of fabricated hybrid rTE/α-elastin hydrogels is lower than bis(sulfosuccinimidyl) suberate (BS3) cross-linked rTE hydrogels reported to be 220–280 kPa [11]. This is likely to be due to the different types of cross-linkers used to produce the elastin-based hydrogels. BS3 cross-linking gives a defined cross-link distance whereas GA can polymerise giving rise to a range of cross-link sizes which could account for the increased stiffness in BS3 cross-linked constructs. The hydrogels fabricated from pure rTE could be extended to strains approximately 90% before breaking, comparable to extensibilities previously reported for aortic elastin (103%) [33].

3.6. In vitro fibroblast cell proliferation using composite rTE/α-elastin hydrogels

One of the important functions of tissue engineering scaffold is to provide a physical support for the cellular growth [36]. Scaffold

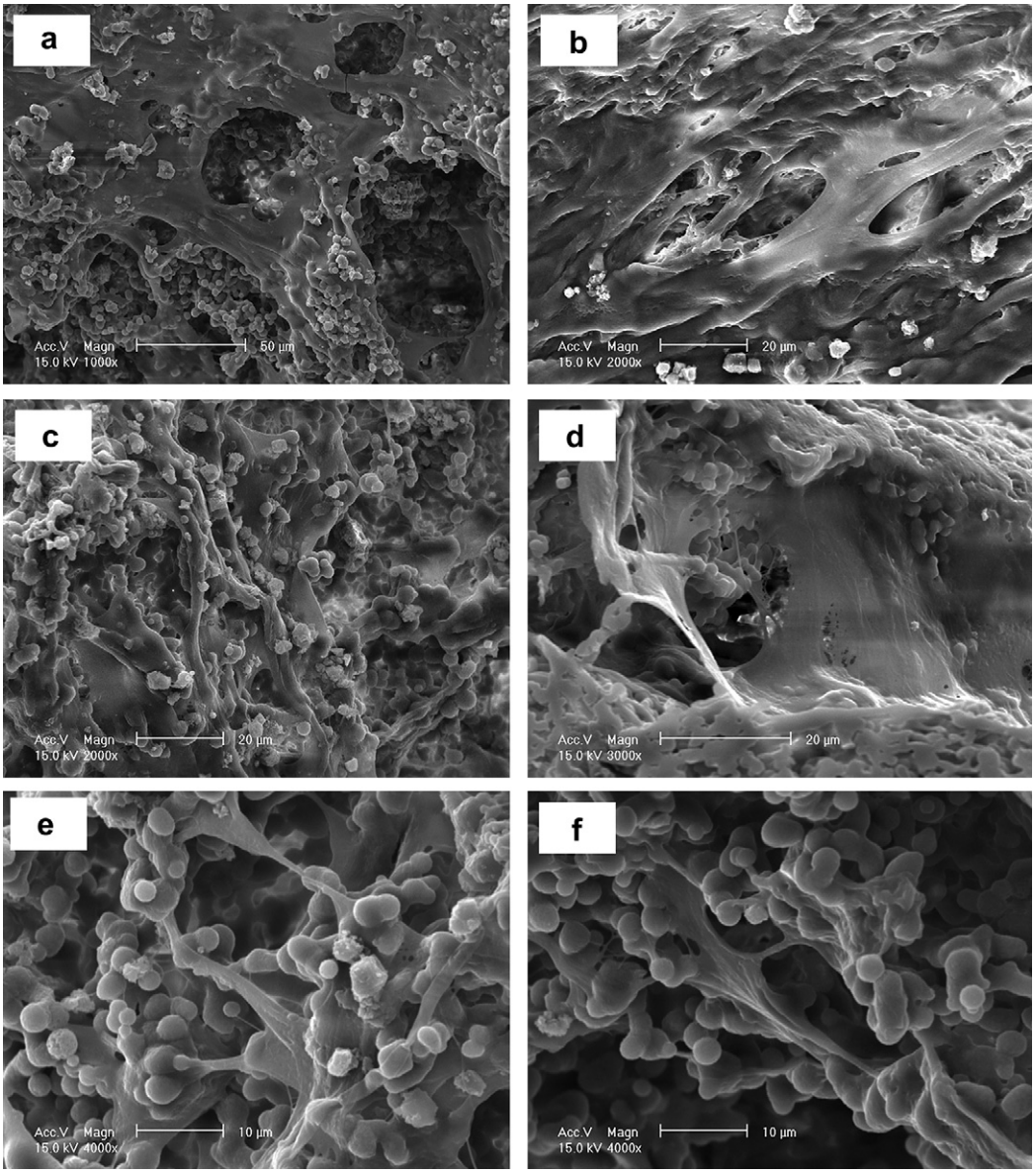

Fig. 10. SEM images of fibroblast cells attached to 50/50 rTE/α-elastin hydrogel fabricated at (a) atmospheric conditions, (b–f) high pressure CO_2. Panel a, b, and c show hydrogel surfaces and panel d–f show hydrogel cross-sections.

microstructure including porosity, mean pore size, and interconnectivity impacts on cell infiltration and proliferation within scaffolds [37–40]. The low surface porosity of hydrogels allows for only a low diffusive flux of nutrients and gas inhibiting cellular growth into the 3D matrices. Without using an intrinsic capillary network, the maximum penetration of cells is approximately 150–200 μm because of the lack of oxygen within the deeper compartments of the biomaterial [41]. In addition, mean pore size has been shown to impact on the amount of contraction a graft will undergo following implantation. An average pore diameter of 20–125 μm was required for contraction inhibiting activity to be observed in a collagen-glycosaminoglycan (CG) graft copolymers used for dermal repair [42].

With pore sizes of 78 ± 17 μm and a compressive modulus more than six-fold greater than that of α-elastin the 50/50 rTE/α-elastin hydrogels were therefore chosen to examine the cell interactive capabilities of the hybrid hydrogels. Human fibroblast cells grew on the top surfaces or slightly penetrate into the SE hydrogel after at least 14 day incubation due to the insufficient pore sizes for cellular growth into the matrices [14]. Cellular growth and proliferation in rTE/α-elastin hybrid hydrogels were examined by light microscopy and SEM analysis to demonstrate the feasibility of using the processed materials as a 3D hydrogel for soft tissue engineering applications. Histology staining of adherent fibroblast cells cultured on hybrid hydrogels produced at high pressure and atmospheric conditions are shown in Fig. 9. As shown in Fig. 9a and c, fibroblast cells proliferated on the surfaces and also penetrated up to approximately 300 μm into rTE/α-elastin hydrogels produced at high pressure. This was due to the presence of large pores, induced by high pressure CO_2, in these constructs. However, cells were only able to form a monolayer on the surface of hydrogels fabricated at atmospheric conditions (Fig. 9b and d). This is likely due to the inability of fibroblast cells to migrate between the small and discontinuous pore networks of samples produced at atmospheric pressure. The SEM images in Fig. 10 confirm the cell proliferation into the 3D structure of hydrogel fabricated at high pressure CO_2. As shown in Fig. 10, cells were able to attach and proliferate on the top surface (Fig. 10b and c) and also into the 3D structure (Fig. 10d–f) of

rTE/α-elastin hydrogels produced under high pressure CO_2 due to the presence of large pores within the materials. However, for the composite hydrogels produced at atmospheric pressure, cells only attach and proliferate across the surface as shown in Fig. 10a.

4. Conclusions

We have previously reported on the structural and cell-supportive properties of hydrogels produced from α-elastin using dense gas technology in an aqueous based system. However, we were unable to report on the mechanical properties of those fabricated hydrogels due to their weak mechanical integrity. The results of this study demonstrate that addition of rTE significantly promoted the properties of elastin hydrogels. The degree of cross-linking was substantially increased when high pressure CO_2 was used during the hydrogel formation; resulting in enhanced mechanical strength and decreased swelling ratio. The use of high pressure CO_2 circumvents the issue of skin formation on the top surfaces of fabricated hydrogels; large pores were generated on the surfaces and within the hybrid hydrogels that facilitated cell proliferation into the 3D structures. The fabricated rTE/α-elastin hydrogels can be contemplated as an elastic biomaterial for soft tissue repair applications.

Acknowledgements

The authors acknowledge financial support from Sydnovate, the Australian Research Council, and Merck Pty Ltd. The authors thank the Graduate School of Biomedical Engineering at University of New South Wales and the School of Aerospace, Mechatronic, & Mechanical Engineering at University of Sydney for access to mechanical testing equipment.

Appendix

Figures with essential colour discrimination. Figs. 1, 7, 8 and 9 of this article may be difficult to interpret in black and white. The full colour images can be found in the on-line version, at doi:10.1016/j.biomaterials.2009.11.051.

References

[1] Langer RS, Vacanti JP. Tissue engineering. Science 1993;260(5110):920–6.
[2] Ma PX. Biomimetic materials for tissue engineering. Adv Drug Deliv Rev 2008;60(2):184–98.
[3] Peppas NA, Hilt JZ, Khademhosseini A, Langer R. Hydrogels in biology and medicine: from molecular principles to bionanotechnology. Adv Mater 2006;18(11):1345–60.
[4] Malafaya PB, Silva GA, Reis RL. Natural-origin polymers as carriers and scaffolds for biomolecules and cell delivery in tissue engineering applications. Adv Drug Deliv Rev 2007;59(4–5):207–33.
[5] Mithieux SM, Weiss AS. Elastin. Fibrous Proteins: Coiled-Coils, Collagen and Elastomers. Adv Protein Chem 2005;70:437–61.
[6] Daamen WF, Veerkamp JH, van Hest JCM, van Kuppevelt TH. Elastin as a biomaterial for tissue engineering. Biomaterials 2007;28(30):4378–98.
[7] Annabi N, Mithieux SM, Boughton EA, Ruys AJ, Weiss AS, Dehghani F. Synthesis of highly porous crosslinked elastin hydrogels and their interaction with fibroblasts in vitro. Biomaterials 2009;30:4550–7.
[8] Leach JB, Wolinsky JB, Stone PJ, Wong JY. Crosslinked alpha-elastin biomaterials: towards a processable elastin mimetic scaffold. Acta Biomater 2005;1(2):155–64.
[9] Annabi N, Mithieux SM, Weiss AS, Dehghani F. The fabrication of elastin-based hydrogels using high pressure CO_2. Biomaterials 2009;30(1):1–7.
[10] Mithieux Suzanne M, Tu Y, Korkmaz E, Braet F, Weiss Anthony S. In situ polymerization of tropoelastin in the absence of chemical cross-linking. Biomaterials 2009;30(4):431–5.
[11] Mithieux SM, Rasko JEJ, Weiss AS. Synthetic elastin hydrogels derived from massive elastic assemblies of self-organized human protein monomers. Biomaterials 2004;25(20):4921–7.
[12] Lim DW, Nettles DL, Setton LA, Chilkoti A. In situ cross-linking of elastin-like polypeptide block copolymers for tissue repair. Biomacromolecules 2008;9(1):222–30.
[13] Vrhovski B, Weiss AS. Biochemistry of tropoelastin. Eur J Biochem 1998;258(1):1–18.
[14] Rnjak J, Li Z, Maitz PKM, Wise SG, Weiss AS. Primary human dermal fibroblast interactions with open weave three-dimensional scaffolds prepared from synthetic human elastin. Biomaterials 2009;30(32):6469–77.
[15] Quirk RA, France RM, Shakesheff KM, Howdle SM. Supercritical fluid technologies and tissue engineering scaffolds. Curr Opin Solid State Mater Sci 2005;8(3–4):313–21.
[16] Tai H, Popov VK, Shakesheff KM, Howdle SM. Putting the fizz into chemistry: applications of supercritical carbon dioxide in tissue engineering, drug delivery and synthesis of novel block copolymers. Biochem Soc Trans 2007;35(3):516–21.
[17] Cansell F, Aymonier C, Loppinet-Serani A. Review on materials science and supercritical fluids. Curr Opin Solid State Mater Sci 2003;7(4–5):331–40.
[18] Barry JJA, Gidda HS, Scotchford CA, Howdle SM. Porous methacrylate scaffolds: supercritical fluid fabrication and in vitro chondrocyte responses. Biomaterials 2004;25(17):3559–68.
[19] Bing Z, Lee JY, Choi SW, Kim JH. Preparation of porous $CaCO_3$/PAM composites by CO_2 in water emulsion templating method. Eur Polym J 2007;43(11):4814–20.
[20] Palocci C, Barbetta A, La Grotta A, Dentini M. Porous biomaterials obtained using supercritical CO_2-water emulsions. Langmuir 2007;23(15):8243–51.
[21] Lee J-Y, Tan B, Cooper AI. CO_2-in-water emulsion-templated poly(vinyl alcohol) hydrogels using poly(vinyl acetate)-based surfactants. Macromolecules 2007;40(6):1955–61.
[22] Partap S, Rehman I, Jones JR, Darr JA. Supercritical carbon dioxide in water emulsion-templated synthesis of porous calcium alginate hydrogels. Adv Mater 2006;18(4):501–4.
[23] Tan B, Lee J-Y, Cooper AI. Synthesis of emulsion-templated poly(acrylamide) using CO_2-in-water emulsions and poly(vinyl acetate)-based block copolymer surfactants. Macromolecules 2007;40(6):1945–54.
[24] Chen C-F, Chang C-S, Chen Y-P, Lin T-S, Su C-Y, Lee S-Y. Applications of supercritical fluid in alloplastic bone graft: a novel method and in vitro tests. Ind Eng Chem Res 2006;45(10):3400–5.
[25] Shih H-h, Lee K-r, Lai H-m, Tsai C-c, Chang Y-c, inventors. Production of porous biodegradable polymers using supercritical fluid. US Patent No. 0064156; 2003.
[26] Annabi N, Mithieux SM, Anthony SW, Dehghani F. Development and characterisation of a novel elastin hydrogel. Mater Res Soc Symp Proc 2009;1140.
[27] Wu WJ, Vrhovski B, Weiss AS. Glycosaminoglycans mediate the coacervation of human tropoelastin through dominant charge interactions involving lysine side chains. J Biol Chem 1999;274(31):21719–24.
[28] Srokowski EM, Woodhouse KA. Development and characterisation of novel cross-linked bio-elastomeric materials. J Biomater Sci Polym Ed 2008;19(6):785–99.
[29] Stammen JA, Williams S, Ku DN, Guldberg RE. Mechanical properties of a novel PVA hydrogel in shear and unconfined compression. Biomaterials 2001;22(8):799–806.
[30] Joshi A, Fussell G, Thomas J, Hsuan A, Lowman A, Karduna A, et al. Functional compressive mechanics of a PVA/PVP nucleus pulposus replacement. Biomaterials 2006;27(2):176–84.
[31] Dehghani F, Annabi N, Valtchev P, Mithieux SM, Weiss AS, Kazarian SG, et al. Effect of dense gas CO_2 on the coacervation of elastin. Biomacromolecules 2008;9(4):1100–5.
[32] Gosline J, Lillie M, Carrington E, Guerette P, Ortlepp C, Savage K. Elastic proteins: biological roles and mechanical properties. Philos Trans R Soc Lond B Biol Sci 2002;357(1418):121–32.
[33] Bellingham CM, Lillie MA, Gosline JM, Wright GM, Starcher BC, Bailey AJ, et al. Recombinant human elastin polypeptides self-assemble into biomaterials with elastin-like properties. Biopolymers 2003;70(4):445–55.
[34] Vieth S, Bellingham CM, Keeley FW, Hodge SM, Rousseau D. Microstructural and tensile properties of elastin-based polypeptides crosslinked with genipin and pyrroloquinoline quinone. Biopolymers 2007;85(3):199–206.
[35] Nickerson MT, Farnworth R, Wagar E, Hodge SM, Rousseau D, Paulson AT. Some physical and microstructural properties of genipin-crosslinked gelatin-maltodextrin hydrogels. Int J Biol Macromol 2006;38(1):40–4.
[36] Liu C, Xia Z, Czernuszka JT. Design and development of three-dimensional scaffolds for tissue engineering. Chem Eng Res Des 2007;85(A7):1051–64.
[37] O'Brien FJ, Harley BA, Yannas IV, Gibson LJ. The effect of pore size on cell adhesion in collagen-GAG scaffolds. Biomaterials 2005;26(4):433–41.
[38] Zeltinger J, Sherwood JK, Graham DA, Mueller R, Griffith LG. Effect of pore size and void fraction on cellular adhesion, proliferation, and matrix deposition. Tissue Eng 2001;7(5):557–72.
[39] Nehrer S, Breinan HA, Ramappa A, Young G, Shortkroff S, Louie LK, et al. Matrix collagen type and pore size influence behavior of seeded canine chondrocytes. Biomaterials 1997;18(11):769–76.
[40] Wake MC, Patrick Jr CW, Mikos AG. Pore morphology effects on the fibrovascular tissue growth in porous polymer substrates. Cell Transplant 1994;3(4):339–43.
[41] Fidkowski C, Kaazempur-Mofrad MR, Borenstein J, Vacanti JP, Langer R, Wang Y. Endothelialized microvasculature based on a biodegradable elastomer. Tissue Eng 2005;11(1–2):302–9.
[42] Yannas IV, Lee E, Orgill DP, Skrabut EM, Murphy GF. Synthesis and characterization of a model extracellular matrix that induces partial regeneration of adult mammalian skin. Proc Natl Acad Sci U S A 1989;86:933–7.
[43] Welsh ER, Tirrell DA. Engineering the extracellular matrix: a novel approach to polymeric biomaterials. I. Control of the physical properties of artificial protein matrices designed to support adhesion of vascular endothelial cells. Biomacromolecules 2000;1(1):23–30.

[44] Nowatzki PJ, Tirrell DA. Physical properties of artificial extracellular matrix protein films prepared by isocyanate crosslinking. Biomaterials 2003;25(7–8):1261–7.
[45] Di Zio K, Tirrell DA. Mechanical properties of artificial protein matrixes engineered for control of cell and tissue behavior. Macromolecules 2003; 36(5):1553–8.
[46] Trabbic-Carlson K, Setton LA, Chilkoti A. Swelling and mechanical behaviors of chemically cross-linked hydrogels of elastin-like polypeptides. Biomacromolecules 2003;4(3):572–80.
[47] Lim DW, Nettles DL, Setton LA, Chilkoti A. Rapid cross-linking of elastin-like polypeptides with (hydroxymethyl)phosphines in aqueous solution. Biomacromolecules 2007;8(5):1463–70.
[48] Iatridis JC, Setton LA, Weidenbaum M, Mow VC. Alterations in the mechanical behavior of the human lumbar nucleus pulposus with degeneration and aging. J Orthop Res 1997;15:318–22.
[49] Zou Y, Zhang Y. An experimental and theoretical study on the anisotropy of elastin network. Ann Biomed Eng 2009;37:1572–83.